

Impact of Recent RHIC Data on Helicity-Dependent Parton Distribution Functions

Emanuele R. Nocera*

*Rudolf Peierls Centre for Theoretical Physics, University of Oxford,
1 Keble Road, OX1 3NP, Oxford, United Kingdom*

(Dated: November 14, 2021)

I study the impact of recent measurements performed at the Relativistic Heavy Ion Collider on the determination of helicity-dependent parton distribution functions of the proton. Specifically, I consider: preliminary data on longitudinally single-spin asymmetries for W -boson production recorded by the STAR experiment during the 2013 run at a center-of-mass energy $\sqrt{s} = 510$ GeV; data on longitudinally double-spin asymmetries for di-jet production recorded by the STAR experiment during the 2009 run at $\sqrt{s} = 200$ GeV; and data on longitudinally double-spin asymmetries for neutral pion production recorded by the PHENIX experiment during a series of runs between 2006 and 2013 at $\sqrt{s} = 200$ GeV and $\sqrt{s} = 510$ GeV. The impact of the new data is studied by applying Bayesian reweighting to NNPDFpol1.1, the most recent global analysis of helicity-dependent parton distribution functions based on the NNPDF methodology. In comparison to NNPDFpol1.1, a slightly more positive polarized gluon PDF, extended to somewhat smaller values of momentum fractions with narrower uncertainties, as well as a slightly more marked and more precise asymmetry between polarized up and down sea quarks are found in this study.

PACS numbers: 3.88.+e, 12.38.Bx, 13.60.Hb, 13.85.Ni

Keywords: Helicity parton distribution functions, Proton spin, Polarized gluons and sea quarks

The Relativistic Heavy Ion Collider (RHIC) at Brookhaven National Laboratory [1] is the only high-energy accelerator ever built which can collide polarized proton beams. This unique feature provides an unprecedented opportunity to investigate how the spin structure of the proton emerges from the interactions among its partonic constituents, in the established framework of perturbative Quantum Chromodynamics (QCD) [2].

One of the main goals of the RHIC spin physics program [3] is to investigate the amount of proton's polarization carried by gluons and sea quarks. This information is encoded in the helicity-dependent (or polarized) Parton Distribution Functions (PDFs)

$$\Delta f(x, \mu^2) \equiv f^\uparrow(x, \mu^2) - f^\downarrow(x, \mu^2), \quad (1)$$

which are defined as the net densities of partons (f denotes either a quark, q , an antiquark, \bar{q} or a gluon, g), with spin aligned along (\uparrow) or opposite (\downarrow) the polarization direction of the parent nucleon, carrying a fraction x of its momentum. Following factorization [4], measured observables are built up as a convolution product between hard-scattering matrix elements and PDFs, which encapsulate respectively the short- and long-distance parts of the interaction. The former can be computed in perturbative QCD, while the latter cannot. Nevertheless, perturbative QCD corrections lead PDFs to depend on the factorization scale μ , as dictated by evolution equations [5]. Provided a suitable set of measurements, usually from a variety of hard-scattering processes, and the corresponding kernels, one should then be able to determine the PDFs from the data in a global QCD analysis.

Some of the leading processes which are being investigated at RHIC include W -boson, jet and pion production in collisions where only one or both proton beams are longitudinally polarized. The corresponding measured observables are single- and double-spin asymmetries,

$$A_L = \frac{\sigma^+ - \sigma^-}{\sigma^+ + \sigma^-} \quad A_{LL} = \frac{\sigma^{++} - \sigma^{+-}}{\sigma^{++} + \sigma^{+-}}, \quad (2)$$

defined as the ratio of the difference to the sum of cross sections with opposite polarizations of one proton beam (+ and - denote the proton beam polarization along or opposite its momentum in the center-of-mass frame).

On the one hand, the production of a jet or a pion arises mainly from gluon-initiated partonic subprocesses. Therefore, a measurement of the associated longitudinal spin asymmetry provides a powerful probe of Δg , the polarized gluon PDF. Such a probe is particularly relevant, because Δg is left almost unconstrained by measurements in fixed-target polarized lepton-nucleon scattering, where it enters the corresponding cross section only via higher-order corrections and scaling violations in the evolution.

On the other hand, the production of a W boson is driven by a purely weak interaction which, because of its chiral nature, couples left-handed quarks with right-handed antiquarks. Therefore, a measurement of the associated longitudinal spin asymmetry provides a clean probe of the flavor decomposition into Δu , $\Delta \bar{u}$, Δd and $\Delta \bar{d}$ PDFs. Such a probe is particularly relevant, because in fixed-target polarized lepton-nucleon scattering quark and antiquark PDFs can be accessed only if the process is semi-inclusive. One exploits correlations between the type of hadron produced in the final state and the flavor of its partonic progenitor. These correlations are expressed by Fragmentation Functions (FFs), which however are on the same footing as PDFs and can limit the accuracy in the description of the process.

* emanuele.nocera@physics.ox.ac.uk

In 2014, a first round of measurements recorded by RHIC [3] were combined with the data from fixed-target lepton-nucleon scattering in two separate next-to-leading order (NLO) global QCD analyses: DSSV14 [6] and NNPDFpol1.1 [7]. They upgraded the corresponding previous analyses, DSSV08 [8] and NNPDFpol1.0 [9], which were based respectively on inclusive and semi-inclusive deep-inelastic scattering (DIS) data, supplemented with a small amount of preliminary RHIC data up to 2005, and on inclusive DIS data only. In both the DSSV14 and NNPDFpol1.0 analyses, single-inclusive jet production asymmetries, measured by the STAR experiment during the 2005-2006 [10] and 2009 [11] runs at a center-of-mass energy $\sqrt{s} = 200$ GeV, were included. Moreover, neutral pion production asymmetries, measured by the PHENIX experiment during the 2006 run at $\sqrt{s} = 62.4$ GeV [12] and at $\sqrt{s} = 200$ GeV [13], as well as during the 2009 run at $\sqrt{s} = 200$ GeV [14], were included in the DSSV14 analysis; W -boson production asymmetries, measured by the STAR experiment during the 2010-2011 runs at $\sqrt{s} = 500$ GeV and $\sqrt{s} = 510$ GeV [15], were included in the NNPDFpol1.1 analysis. Neutral pion production asymmetries were not included in NNPDFpol1.1 because, like semi-inclusive fixed-target DIS data, they entail the knowledge of FFs. Such a knowledge has significantly improved since then, at least for pions. Several new global QCD analyses of FFs have been performed recently with a bunch of very precise data from B -factories [16], including the first analysis based on the same methodology adopted in NNPDFpol1.1 [17]. It would then be interesting to revisit neutral pion production at RHIC in light of these new developments.

Both the DSSV14 and NNPDFpol1.1 analyses have shown the substantial impact of RHIC measurements in improving our knowledge of polarized PDFs [18]. Indeed, they revealed for the first time a sizable, positive polarization of gluons (in both analyses similar results were found despite the different data set included), and a sizable, positive asymmetry between polarized up and down sea quarks (in the NNPDFpol1.1 analysis, thanks to W -boson production data).

Since then, some new experimental measurements have become available from RHIC. In this contribution, I study the impact of some of them in the framework of a global analysis based on the NNPDF methodology. Specifically, I focus on the following sets of data.

First, I consider preliminary measurements [19] of the single-spin asymmetry for W -boson production, A_L^W , recorded by the STAR experiment during the 2013 run at $\sqrt{s} = 510$ GeV. The integrated luminosity of the sample is $\mathcal{L} = 246.2$ pb $^{-1}$. Asymmetries are provided separately for W^+ and W^- final states, which were reconstructed from their $W^\pm \rightarrow e^\pm \nu$ decay channels, as a function of the decay electron/positron rapidity η^{e^\pm} . The data is presented in four bins for W^+ and four bins for W^- and is integrated over the electron/positron transverse momentum in the range $25 \text{ GeV} < p_T^{e^\pm} < 50 \text{ GeV}$. Using leading-order (LO) kinematics, one can expect this data

to constrain polarized quark and antiquark PDFs with $0.05 \lesssim x \lesssim 0.4$ and $\mu \sim M_W$, where M_W is the mass of the W boson. The uncertainties of the data are mainly statistical, though they are reduced by about 40% with respect to the previous measurements taken during the 2010-2011 runs. In the experimental analysis, they are combined with systematic uncertainties due to the unpolarized background dilutions. Additional subdominant correlated systematics, originating from the beam polarization (3.3% of the asymmetry) and from the relative luminosity (an offset of 0.004 on the asymmetry), are provided separately.

Second, I consider the first measurement [20] of the double-spin asymmetry for mid-rapidity di-jet production, $A_{LL}^{2\text{jets}}$, recorded by the STAR experiment during the 2009 run at $\sqrt{s} = 200$ GeV. The integrated luminosity of the sample is $\mathcal{L} = 21$ pb $^{-1}$. In the experimental analysis, di-jets events were selected by choosing the two jets with the highest transverse momentum $p_{T;1,2}$ from a single event that fell in the range $-0.8 \leq \eta_{1,2} \leq 0.8$, with $\eta_{1,2}$ the rapidity of each of the two jets. Furthermore, an asymmetric condition was placed on the transverse momentum of each of the two jets, specifically $p_{T;1} \geq 8.0$ GeV and $p_{T;2} \geq 6.0$ GeV. The jet reconstruction procedures followed those used in the previous single-inclusive jet analysis [11], including the usage of the anti- k_T algorithm [21] for jet finding (with resolution parameter $R = 0.6$). Asymmetries are provided as a function of the invariant mass of the di-jet pair, $M^{2\text{jets}}$, for two distinct topologies in seven bins each: *same-sign*, in which both jets have either positive or negative rapidities, and *opposite-sign*, in which one jet has positive and the other has negative rapidity. The opposite-sign topology selects events arising from relatively symmetric (in x) partonic collisions, whereas same-sign events select more asymmetric collisions. Using LO kinematics, one can expect this data to constrain the polarized gluon PDF with $0.01 \lesssim x \lesssim 0.2$ and $\mu \sim M^{2\text{jets}}$, where $15 \text{ GeV} \lesssim M^{2\text{jets}} \lesssim 70 \text{ GeV}$. The uncertainties on the data are dominated by statistics. A full breakdown of systematics is also provided, along with the correlation matrix for the quadrature sum of the point-to-point statistical and systematic uncertainties between single- and di-jet asymmetries from the 2009 run. There are two additional systematics, which are 100% correlated among bins, originating from the beam polarization (6.5% of the asymmetry) and from the relative luminosity (an offset of 5×10^{-4} on the asymmetry).

Third, I consider measurements of the double-spin asymmetry for mid-rapidity neutral pion production, $A_{LL}^{\pi^0}$, recorded by the PHENIX experiment during the 2009 run at $\sqrt{s} = 200$ GeV (and combined with previous 2005 and 2006 runs at the same center-of-mass energy) [14], and the 2012-2013 runs at $\sqrt{s} = 510$ GeV [22]. The integrated luminosity of the samples are $\mathcal{L} = 6.5$ pb $^{-1}$ (for the 2009 run), $\mathcal{L} = 20$ pb $^{-1}$ (for the 2012 run) and $\mathcal{L} = 108$ pb $^{-1}$ (for the 2013 run). The data is presented in ten bins, for the asymmetries at $\sqrt{s} = 200$ GeV,

TABLE I. The data sets considered in this analysis. For each set, I indicate the name adopted to denote it, the corresponding publication reference, the integrated luminosity, \mathcal{L} , the center-of-mass energy, \sqrt{s} , the measured asymmetry, \mathcal{A} , and the number of data points, N_{dat} .

Data set	Ref.	\mathcal{L} [pb $^{-1}$]	\sqrt{s} [GeV]	\mathcal{A}	N_{dat}
STAR13- W^-	[19]	246.2	510	$A_L^{e^-}$	4
STAR13- W^+	[19]	246.2	510	$A_L^{e^+}$	4
STAR09-2j-ss	[20]	21	200	$A_{LL}^{2\text{jets}}$	7
STAR09-2j-os	[20]	21	200	$A_{LL}^{2\text{jets}}$	7
PHENIX09- π^0	[14]	6.5	200	$A_{LL}^{\pi^0}$	12
PHENIX13- π^0	[22]	128	510	$A_{LL}^{\pi^0}$	14

and in fourteen bins, for the asymmetries at $\sqrt{s} = 510$ GeV, as a function of the transverse momentum of the final neutral pion, $p_T^{\pi^0}$. The rapidity coverage of the detector is $|\eta| < 0.35$. Using LO kinematics, one can expect this data to constrain the polarized gluon PDF with $0.05 \lesssim x \lesssim 0.2$ when $\sqrt{s} = 200$ GeV ($0.01 \lesssim x \lesssim 0.2$ when $\sqrt{s} = 510$ GeV) and $\mu \sim p_T^{\pi^0}$, where $1 \text{ GeV} \lesssim p_T^{\pi^0} \lesssim 17 \text{ GeV}$. The uncertainties on the data are dominated by statistics, except for small- $p_T^{\pi^0}$ bins. There are two bin-by-bin fully correlated systematics originating from the beam polarization (4.8% and 6.5% of the asymmetry at $\sqrt{s} = 200$ GeV and $\sqrt{s} = 510$ GeV respectively) and from the relative luminosity (an offset of 4.2×10^{-4} and 3.6×10^{-4} on the asymmetry at $\sqrt{s} = 200$ GeV and $\sqrt{s} = 510$ GeV respectively).

Here, I do not consider other recent measurements performed at RHIC, specifically neutral pion production asymmetries measured by STAR at $\sqrt{s} = 200$ GeV [23] and $\sqrt{s} = 510$ GeV [24], and W -boson production asymmetries measured by PHENIX at $\sqrt{s} = 500$ GeV and $\sqrt{s} = 510$ GeV [25]. This data is affected by rather large uncertainties, which are likely to limit its impact on PDFs [7]. The data sets considered in this analysis are summarized in Tab. I, where I indicate, for each of them, the name adopted to denote them, their corresponding publication reference, the integrated luminosity, \mathcal{L} , the center-of-mass energy, \sqrt{s} , the measured asymmetry, \mathcal{A} , and the number of data points, N_{dat} .

In Figs. 1-2-3, I compare the measured asymmetries for each of the data sets collected in Tab. I with the corresponding theoretical predictions. The latter have all been computed at NLO accuracy in perturbative QCD. They have been obtained using the NNPDFpol1.1 parton set [7] for polarized PDFs and the NNPDF3.0 parton set [26] for unpolarized PDFs. In the case of neutral pion production asymmetries, the preliminary NNFF1.0 parton set [17] has been used for FFs. All used sets are NLO. The uncertainties on the theoretical predictions displayed in Figs. 1-2-3 are one-sigma bands. They have been computed by propagating the uncertainty on the polarized

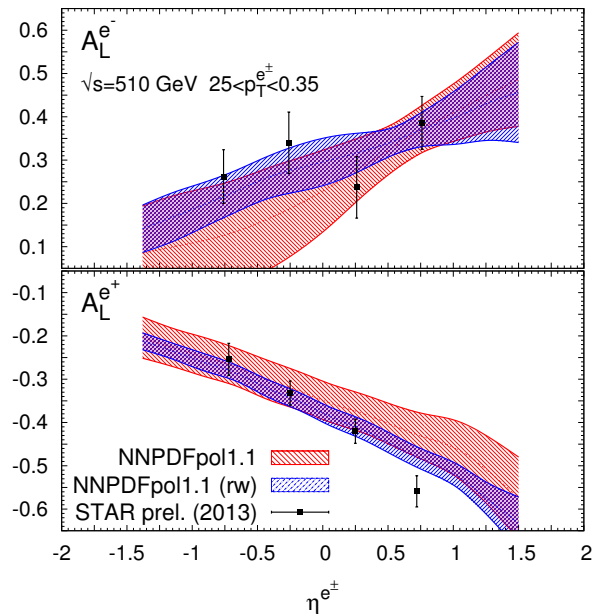


FIG. 1. The electron (top) and positron (bottom) single-spin asymmetry for W^- and W^+ production in single-polarized proton-proton collisions at $\sqrt{s} = 510$ GeV, as a function of the decay electron/positron rapidity η^{e^\pm} . The data is from preliminary STAR measurements taken during the 2013 run [19]. Displayed data uncertainties are statistical only. Theoretical predictions are computed at NLO with the NNPDFpol1.1 polarized PDF set and the NNPDF3.0 unpolarized PDF set. Results are shown before and after reweighting with the corresponding data. One-sigma uncertainty bands reflect uncertainties from the input polarized PDFs only.

PDFs only, while unpolarized PDFs and FFs have been set to their central values. This is justified because, in the kinematic region where asymmetries are measured, the unpolarized PDF and FF uncertainties are subdominant with respect to the polarized PDF uncertainty. Furthermore, in the case of neutral pion production asymmetries, I have explicitly checked that almost indistinguishable predictions are obtained with either the NNFF1.0 or the DSS15 [16] FF sets. Theoretical predictions have been computed by using the following pieces of code, which have been modified to handle NNPDF parton sets. For W -boson production, I have used the code of Ref. [27]; for di-jet production, I have used the code of Ref. [28], supplemented with the FastJet Package [29]; for neutral pion production, I have used the code of Ref. [30].

The agreement between the data and theoretical predictions is quantified by the χ^2 per data point, χ^2/N_{dat} , which is displayed in the third column of Tab. II. This is computed by taking into account all the available information on statistical and systematic uncertainties, including their correlations, when the experimental covariance matrix is constructed. From Tab. II and Figs. 1-2-3, NLO theoretical predictions based on NNPDF parton sets do appear to provide a good description of di-jet and neu-

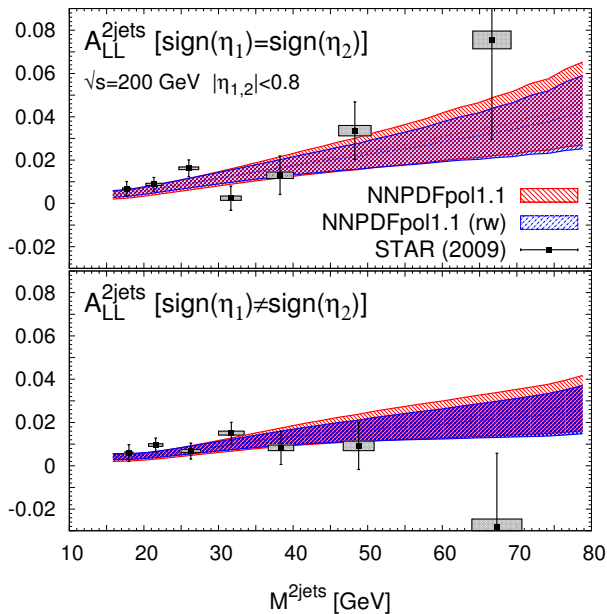


FIG. 2. The double-spin asymmetry with same-sign (top) and opposite-sign (bottom) rapidity topologies for di-jet production in double-polarized proton-proton collisions at $\sqrt{s} = 200$ GeV, as a function of the invariant mass of the di-jet pair, M^{2jets} . The experimental data is from STAR measurements taken during the 2009 run [20]. Statistical and systematic (shaded boxes) data uncertainties are displayed. Theoretical predictions and uncertainties bands are shown as in Fig. 1.

tral pion production double-spin asymmetries, while they do not for W -boson production single-spin asymmetries. This is not unexpected. On the one hand, the NNPDF-pol1.1 set already included jet production data, of which di-jet production data are a subsample. They allowed for a rather accurate determination of the gluon PDF in the same kinematic region where it is sensitive to di-jet and neutral pion production data. On the other hand, the NNPDFpol1.1 set included the STAR 2010-2011 W -boson production data, which had significantly larger uncertainties than the new STAR 2013 data. For di-jet and neutral pion production asymmetries, the size of the uncertainties on theoretical predictions is comparable to (or smaller than) the size of the statistical uncertainties on the data. Conversely, for W -boson production asymmetries, theoretical uncertainties are always larger than data uncertainties. One should then expect the largest impact on the underlying PDFs from the last set of data.

In order to assess the impact of the new RHIC data on the polarized PDFs, I include them in the NNPDF-pol1.1 parton set by means of Bayesian reweighting [31]. This methodology consists in updating the representation of the probability distribution in the space of PDFs - provided by a *prior* Monte Carlo ensemble of equally probable PDFs - by means of Bayes' theorem. Specifically, each replica in the prior set is assigned a weight which assesses the probability that this replica agrees

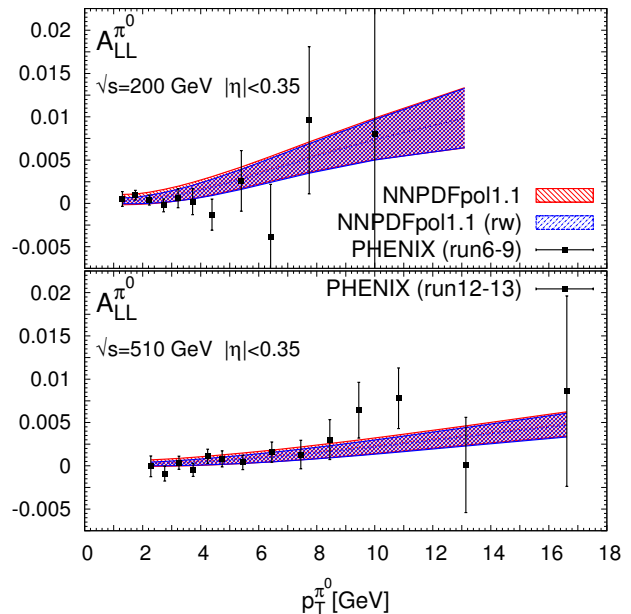


FIG. 3. The double-spin asymmetry for neutral pion production in double-polarized proton-proton collisions at $\sqrt{s} = 200$ GeV from PHENIX measurements taken during the 2005-2006-2009 runs (top) and at $\sqrt{s} = 510$ GeV from PHENIX measurements taken during the 2012-2013 runs (bottom). Results are displayed as a function of the neutral pion transverse momentum $p_T^{\pi^0}$. Displayed data uncertainties are statistical only. Theoretical predictions and uncertainties bands are shown as in Fig. 1. The NNFF1.0 set of FFs [17] is used.

TABLE II. The values of the χ^2 per data point, χ^2/N_{dat} ($\chi_{\text{rw}}^2/N_{\text{dat}}$), before (after) reweighting, the effective number of replicas, N_{eff} , and the modal value of the $\mathcal{P}(\alpha)$ distribution, $\langle\alpha\rangle$, for each data set with which the NNPDFpol1.1 PDFs are reweighted. The number of data points for each data set, N_{dat} , is displayed for reference.

Data set	N_{dat}	χ^2/N_{dat}	$\chi_{\text{rw}}^2/N_{\text{dat}}$	N_{eff}	$\langle\alpha\rangle$
STAR13- W^-	4	2.44	0.69	38	1.35
STAR13- W^+	4	3.08	1.30	29	1.55
STAR09-2j-ss	7	1.41	1.18	89	1.10
STAR09-2j-os	7	1.26	0.83	92	1.05
PHENIX09- π^0	12	0.69	0.60	84	0.75
PHENIX13- π^0	14	0.61	0.58	92	0.80

with the new data. The weights are computed by evaluating the χ^2 of the new data to the prediction obtained using a given replica. After reweighting, replicas with small weights become almost irrelevant in ensemble averages, and the number of effective replicas in the Monte Carlo ensemble (see Eq. (10) in Ref. [31]) is smaller than the starting one. The consistency of the data used for reweighting with that included in the prior set can be assessed by examining the χ^2 profile of the new data,

$\mathcal{P}(\alpha)$, where α is the factor by which the uncertainty on the new data must be rescaled in order for both the prior and the reweighted sets to be consistent with each other (see Eq. (12) in Ref. [31]). If the modal value of α is close to unity, the new data is consistent with the old, and its uncertainties have been correctly estimated.

I perform a simultaneous reweighting of the NNPDFpol1.1 parton set with all the data sets listed in Tab. I. In Tab. II, I show the values of the χ^2 per data point after reweighting, $\chi^2_{\text{rw}}/N_{\text{dat}}$, the number of effective replicas, N_{eff} , and the modal value of the $\mathcal{P}(\alpha)$ distribution, $\langle\alpha\rangle$. The corresponding asymmetries, after reweighting with the new data, are displayed in Figs. 1-2-3, on top of their counterparts before reweighting.

The value of the χ^2 per data point always decreases after reweighting. The improvement is marked for the W -boson production data, moderate for the di-jet production data and only slight for the neutral pion production data. This is expected, since the first data set has the smallest uncertainties, among all, in comparison to the PDF uncertainties on the theoretical predictions. This suggests that this data is bringing in a significant amount of new information. After reweighting, the χ^2 per data point is of order one for all the new data sets. However, in the case of W -boson and neutral pion production asymmetries, these numbers should be taken with care, because a complete information on correlated systematics is not available. This is the reason why the reweighted χ^2 is smaller than one for these sets, except for the W^+ production data. In this case, the value of the χ^2 is raised by a sizable contribution coming from the point with the largest positron rapidity, which disagrees by about two sigma with the reweighted theoretical prediction and the previous STAR measurement from run 2010-2011 (see also Fig. 4 in ref [19]).

The number of effective replicas after reweighting depends significantly on the data set. The size of the reweighted parton set is about 90% of the original NNPDFpol1.1 parton set (made of $N_{\text{rep}} = 100$ replicas) for di-jet and pion production data, while it is only about 30%-40% for W -boson production data. This result reflects the different constraining power of the various data sets, which is maximized in the last case. In principle, a prior ensemble with a larger number of replicas should then be needed for the reweighted ensemble to sample the probability density in the space of PDFs with as much accuracy. However this is not relevant here, as reweighted results only serve to assess the impact of the new data, and are not used to construct a new parton set.

The modal value of the $\mathcal{P}(\alpha)$ distribution is of order one for all the new data sets. Values of $\langle\alpha\rangle$ slightly larger than one are found for the W -boson production data: in the case of W^- , this is mostly determined by a sizable fluctuation of one data point (around $\eta^{e^-} \sim 0.25$) with respect to the shape of the corresponding asymmetry; in the case of W^+ , this is mostly determined by the fourth data point (around $\eta^{e^+} \sim 0.75$), which, as already noted, disagrees by about two sigma with the reweighted theo-

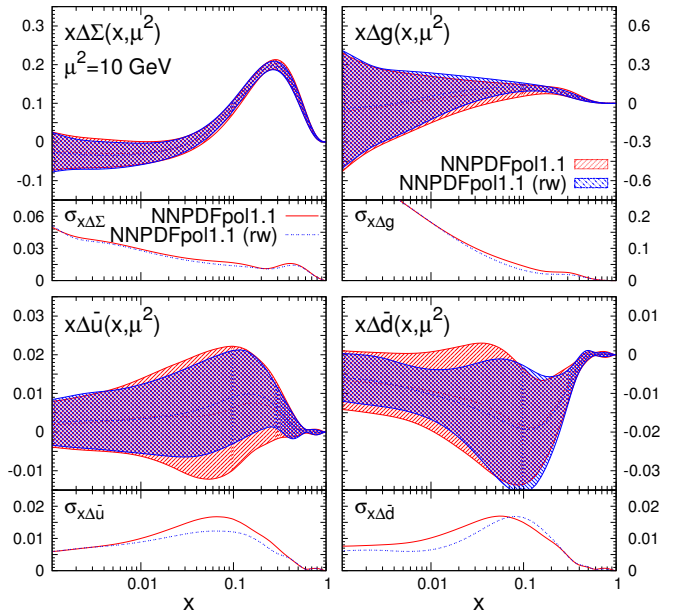


FIG. 4. A comparison of polarized PDFs before and after the simultaneous reweighting of NNPDFpol1.1 with the data sets listed in Tab. I. From left to right, top to bottom, the singlet, $\Delta\Sigma$, the gluon, Δg , and the up and down sea quarks, $\Delta\bar{u}$ and $\Delta\bar{d}$, are displayed. Parton distributions are evaluated at $\mu^2 = 10$ GeV. Bands represent one-sigma uncertainties; they are also shown in the lower inset of each panel.

retical prediction. Values of $\langle\alpha\rangle$ slightly smaller than one are found for the neutral pion production data, thus suggesting that experimental uncertainties are likely to be overestimated, possibly because of the lack of a complete information on correlations among systematics.

In Fig. 4, I compare the polarized PDFs before and after the simultaneous reweighting of NNPDFpol1.1 with the data sets listed in Tab. I. From left to right, top to bottom, I show the singlet (for n_f active flavors), $\Delta\Sigma = \sum_{i=1}^{n_f} (\Delta q_i + \Delta \bar{q}_i)$, the gluon, Δg , and the up and down sea quarks, $\Delta\bar{u}$ and $\Delta\bar{d}$. Parton distributions are evaluated at $\mu^2 = 10$ GeV². Bands represent one-sigma uncertainties, which are also displayed separately in the lower inset of each panel.

The impact of the new data on the polarized PDFs of the proton is twofold. On the one hand, it induces a shift of the PDF central values, as a consequence of the adjustment to the shape of the corresponding asymmetries. Specifically, the central value of Δg increases by about 30% of its original value in the region $0.1 \lesssim x \lesssim 0.2$; the central value of $\Delta\bar{u}$ increases by about 25% and that of $\Delta\bar{d}$ decreases by about 10% approximately in the same region of x where also Δg is affected. On the other hand, the new data induces a reduction of the PDF uncertainties, as a consequence of the improved precision of the corresponding asymmetries. For Δg and $\Delta\bar{d}$ such a reduction is moderate, and not larger than 5% of its original value; for $\Delta\bar{u}$ it is fairly more pronounced, around

25%. As expected, these differences appear in the kinematic region where the PDFs are sensitive to the new data, roughly $0.1 \lesssim x \lesssim 0.2$. Central values and uncertainties of other PDFs, like the singlet or the up, down and strange (not shown in Fig. 4) are not significantly affected by the new data.

The impact of the new data is also revealed by the truncated first moments of the corresponding PDFs in the region $[x_{\min}, x_{\max}]$

$$\langle \Delta f(\mu^2) \rangle^{[x_{\min}, x_{\max}]} \equiv \int_{x_{\min}}^{x_{\max}} dx \Delta f(x, \mu^2). \quad (3)$$

Specifically, Eq. (3) gives, at $\mu^2 = Q^2 = 10 \text{ GeV}^2$, respectively before and after reweighting: $\langle \Delta g(Q^2) \rangle^{[0.01, 0.2]} = 0.23 \pm 0.23$ and $\langle \Delta g(Q^2) \rangle_{\text{rw}}^{[0.01, 0.2]} = 0.32 \pm 0.21$; $\langle \Delta \bar{u}(Q^2) \rangle^{[0.01, 0.2]} = 0.01 \pm 0.04$ and $\langle \Delta \bar{u}(Q^2) \rangle_{\text{rw}}^{[0.01, 0.2]} = 0.02 \pm 0.03$; $\langle \Delta \bar{d}(Q^2) \rangle^{[0.01, 0.2]} = -0.04 \pm 0.04$ and $\langle \Delta \bar{d}(Q^2) \rangle_{\text{rw}}^{[0.01, 0.2]} = -0.05 \pm 0.03$.

In summary, in comparison to the NNPDFpol1.1 anal-

ysis, a slightly more positive polarized gluon PDF, extended to somewhat smaller values of momentum fractions with narrower uncertainties, as well as a slightly more marked and more precise asymmetry between polarized up and down sea quarks are found in this study. These results confirm the importance of the RHIC spin physics program in the understanding of the longitudinal spin structure of the proton.

ACKNOWLEDGMENTS

I would like to thank the organizers of the SPIN2016 conference for the opportunity to be a convener of Working Group B: *Nucleon Helicity Structure* and for financial support. I am also grateful to Sasha Bazilevsky, for discussions on neutral pion production data from the PHENIX experiment, and to Brian Page, for clarifications on systematic uncertainties of di-jet production data from the STAR experiment. This work is supported by a STFC Rutherford Grant ST/M003787/1.

-
- [1] M. Harrison, S. G. Peggs, and T. Roser, *Ann. Rev. Nucl. Part. Sci.* **52**, 425 (2002); M. Harrison, T. Ludlam, and S. Ozaki, *Nucl. Instrum. Meth.* **A499**, 235 (2003).
- [2] G. Bunce, N. Saito, J. Soffer, and W. Vogelsang, *Ann. Rev. Nucl. Part. Sci.* **50**, 525 (2000).
- [3] E.-C. Aschenauer *et al.*, (2015), arXiv:1501.01220 [nucl-ex].
- [4] J. C. Collins, D. E. Soper, and G. F. Sterman, *Adv. Ser. Direct. High Energy Phys.* **5**, 1 (1989).
- [5] V. N. Gribov and L. N. Lipatov, *Sov. J. Nucl. Phys.* **15**, 438 (1972); L. N. Lipatov, *ibid.* **20**, 94 (1975); G. Altarelli and G. Parisi, *Nucl. Phys.* **B126**, 298 (1977); Y. L. Dokshitzer, *Sov. Phys. JETP* **46**, 641 (1977).
- [6] D. de Florian, R. Sassot, M. Stratmann, and W. Vogelsang, *Phys. Rev. Lett.* **113**, 012001 (2014).
- [7] E. R. Nocera, R. D. Ball, S. Forte, G. Ridolfi, and J. Rojo, *Nucl. Phys.* **B887**, 276 (2014).
- [8] D. de Florian, R. Sassot, M. Stratmann, and W. Vogelsang, *Phys. Rev. Lett.* **101**, 072001 (2008); *Phys. Rev.* **D80**, 034030 (2009).
- [9] R. D. Ball, S. Forte, A. Guffanti, E. R. Nocera, G. Ridolfi, and J. Rojo, *Nucl. Phys.* **B874**, 36 (2013).
- [10] L. Adamczyk *et al.*, *Phys. Rev.* **D86**, 032006 (2012).
- [11] L. Adamczyk *et al.*, *Phys. Rev. Lett.* **115**, 092002 (2015).
- [12] A. Adare *et al.*, *Phys. Rev.* **D79**, 012003 (2009).
- [13] A. Adare *et al.*, *Phys. Rev. Lett.* **103**, 012003 (2009).
- [14] A. Adare *et al.*, *Phys. Rev.* **D90**, 012007 (2014).
- [15] L. Adamczyk *et al.*, *Phys. Rev. Lett.* **113**, 072301 (2014).
- [16] D. de Florian, R. Sassot, M. Epele, R. J. Hernandez-Pinto, and M. Stratmann, *Phys. Rev.* **D91**, 014035 (2015); M. Hirai, H. Kawamura, S. Kumano, and K. Saito, *PTEP* **2016**, 113B04 (2016); N. Sato, J. J. Ethier, W. Melnitchouk, M. Hirai, S. Kumano, and A. Accardi, *Phys. Rev.* **D94**, 114004 (2016).
- [17] E. R. Nocera, in *22nd International Symposium on Spin Physics (SPIN 2016) Urbana, IL, USA, September 25-30, 2016* (2017) arXiv:1701.09186 [hep-ph].
- [18] E. R. Nocera, *Proceedings, 21st International Symposium on Spin Physics (SPIN 2014): Beijing, China, October 20-24, 2014*, *Int. J. Mod. Phys. Conf. Ser.* **40**, 1660016 (2016).
- [19] D. Gunarathne, in *22nd International Symposium on Spin Physics (SPIN 2016) Urbana, IL, USA, September 25-30, 2016* (2017) arXiv:1702.02927 [nucl-ex].
- [20] L. Adamczyk *et al.*, (2016), arXiv:1610.06616 [hep-ex].
- [21] M. Cacciari, G. P. Salam, and G. Soyez, *JHEP* **04**, 063 (2008).
- [22] A. Adare *et al.*, *Phys. Rev.* **D93**, 011501 (2016).
- [23] L. Adamczyk *et al.*, *Phys. Rev.* **D89**, 012001 (2014).
- [24] C. J. Dilks, *Proceedings, 21st International Symposium on Spin Physics (SPIN 2014): Beijing, China, October 20-24, 2014*, *Int. J. Mod. Phys. Conf. Ser.* **40**, 1660024 (2016).
- [25] A. Adare *et al.*, *Phys. Rev.* **D93**, 051103 (2016).
- [26] R. D. Ball *et al.*, *JHEP* **04**, 040 (2015).
- [27] D. de Florian and W. Vogelsang, *Phys. Rev.* **D81**, 094020 (2010).
- [28] D. de Florian, S. Frixione, A. Signer, and W. Vogelsang, *Nucl. Phys.* **B539**, 455 (1999).
- [29] M. Cacciari, G. P. Salam, and G. Soyez, *Eur. Phys. J.* **C72**, 1896 (2012).
- [30] B. Jager, A. Schafer, M. Stratmann, and W. Vogelsang, *Phys. Rev.* **D67**, 054005 (2003).
- [31] R. D. Ball, V. Bertone, F. Cerutti, L. Del Debbio, S. Forte, A. Guffanti, J. I. Latorre, J. Rojo, and M. Ubiali, *Nucl. Phys.* **B849**, 112 (2011), [Erratum: *Nucl. Phys.* **B855**, 927(2012)]; R. D. Ball, V. Bertone, F. Cerutti, L. Del Debbio, S. Forte, A. Guffanti, N. P. Hartland, J. I. Latorre, J. Rojo, and M. Ubiali, *Nucl. Phys.* **B855**, 608 (2012).
- [32] A. Adare *et al.*, *Phys. Rev.* **D91**, 032001 (2015).